Surface Profile Reconstruction from Scattered Intensity Data Using Evolutionary Strategies

Demetrio Macías, Gustavo Olague, and Eugenio R. Méndez

División de Física Aplicada,
Centro de Investigación Científica y de Educación Superior de Ensenada,
Apdo. Postal 2732, 22800 Ensenada, B. C., México.
(dmacias, olague, emendez)@cicese.mx

Abstract. We present a study of rough surface inverse scattering problems using evolutionary strategies. The input data consists of far-field angle-resolved scattered intensity data, and the objective is to reconstruct the surface profile function that produced the data. To simplify the problem, the random surface is assumed to be one-dimensional and perfectly conducting. The optimum of the fitness function is searched using the evolutionary strategies (μ, λ) and $(\mu + \lambda)$. On the assumption that some knowledge about the statistical properties of the unknown surface profile is given or can be obtained, the search space is restricted to surfaces that belong to that particular class. In our case, as the original surface, the trial surfaces constitute realizations of a stationary zero-mean Gaussian random process with a Gaussian correlation function. We find that, for the conditions and parameters employed, the surface profile can be retrieved with high degree of confidence. Some aspects of the convergence and the lack of uniqueness of the solution are also discussed.

1 Introduction

The interaction of electromagnetic waves with randomly rough surfaces is a subject of importance in many scientific disciplines. It finds applications, for example, in the remote sensing of the ocean surface and the Earth's terrain, and in studies of astronomical objects with radio waves. In optics, it has applications in surface metrology, in the evaluation of optical components and systems, and in the development of paints and coatings, to mention but a few. The direct scattering problem, that consists of finding the scattered field or the scattered intensity from knowledge of the surface profile, its optical properties, and the conditions of illumination, has been widely studied in the past [1,2]. Approximate methods of solution, such as perturbation theory [2,3] and the use of the Kirchhoff boundary conditions [1,2], have lead to a better understanding of different aspects of the phenomenon, but more rigorous methods [4,5] are required to account for the multiple scattering phenomena that give rise to coherent effects such as that of enhanced backscattering [6,7].

The inverse scattering problem, on the other hand, that consists of the reconstruction of the profile of a surface from scattering data has also received some

S. Cagnoni et al. (Eds.): EvoWorkshops 2002, LNCS 2279, pp. 233–244, 2002.

attention, but due to the difficulties involved little progress has been made. Many of the works on inverse scattering have focused on the retrieval of some statistical properties of the surface under study [8,9,10,11,12]. The reconstruction of surface profiles from far-field amplitude data has been considered by Wombel and DeSanto [13,14], Quartel and Sheppard [15,16], and Macías *et al.* [17]. From a practical stand point, the need to have amplitude, rather than intensity data, constitutes an important drawback that all these methods share. Optical detectors are not phase sensitive; they respond only to intensity and special schemes need to be used to determine the phase of the optical field. The other important limitation is that these methods are based on simple approximate models for the interaction between the incident light and the surface, and fail when multiple scattering is important.

In the present work, the inverse scattering problem is viewed as a problem of constrained optimization. We implement, and study the performance of two inversion algorithms based on evolutionary strategies taking, as the input, far-field intensity data. Unlike previous works on the subject, the method does not rely on approximate expressions for the field-surface interaction. Furthermore, although at present we can not demonstrate this, our experience with the method indicates that the convergence to the optimum improves when multiple scattering occurs. Since, in general, the use of intensity data implies that the solution to the problem is not unique, the improvement in the convergence is possibly due to a reduction in the number of solutions in the presence of multiple scattering.

The organization of this paper is as follows. Section 2 deals with the direct scattering problem. We introduce the notation and discuss the complexity of the relation between the surface profile and the far-field intensity. In Sect. 3, we approach the inverse scattering problem as an optimization problem, describing in some detail the procedure to generate and mutate the surfaces. Some problems occurring when intermediate recombination is employed are also pointed out. Section 4 is devoted to the description of the algorithms studied, and typical results are presented and discussed in Sect. 5. Finally, in Sect. 6, we present our main conclusions.

2 The Direct Scattering Problem

We consider the scattering of light from a one-dimensional, perfectly conducting, randomly rough surface defined by the equation $x_3 = \zeta(x_1)$. The region $x_3 > \zeta(x_1)$ is vacuum, the region $\zeta(x_1) > x_3$ is a perfect conductor, and the plane of incidence is the x_1x_3-plane. With reference to Fig. 1, the surface is illuminated from the vacuum side by an s-polarized plane wave making an angle θ_0 with the x_3 axis.

The scattering amplitude $R_s(q|k)$ can be written in the form [5]

$$R_s(q|k) = \frac{-i}{2\alpha_0(k)} \int_{-\infty}^{\infty} dx_1 \left[\exp\{-i\alpha_0(q)\zeta(x_1)\}F(x_1|\omega)\right] \exp\{-iqx_1\}, \qquad (1)$$

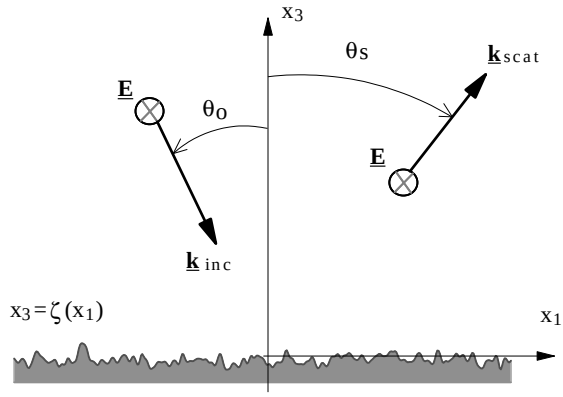

Fig. 1. Geometry of the scattering problem considered.

where

$$F(x_1|\omega) = \left(-\zeta'(x_1)\frac{\partial}{\partial x_1} + \frac{\partial}{\partial x_3}\right) E_2(x_1, x_3)\Big|_{x_3=\zeta(x_1)} \tag{2}$$

represents the source function, $E_2(x_1, x_3)$ is the only nonzero component of the electric field, $\alpha_0(k) = \sqrt{\omega^2/c^2 - k^2}$, and $\alpha_0(q) = \sqrt{\omega^2/c^2 - q^2}$. The angles of incidence θ_0 and scattering θ_s are related to the components of the incident and scattered wavevectors that are parallel to the mean surface through the expressions

$$k = \frac{\omega}{c}\sin\theta_0\,, \qquad\qquad q = \frac{\omega}{c}\sin\theta_s\,, \tag{3}$$

where c is the speed of light and ω is the frequency of the optical field. The far-field intensity $I_s(q|k)$ is defined as the squared modulus of the scattering amplitude $R_s(q|k)$.

At this point, it is important to mention that the source function $F(x_1|\omega)$ is unknown, and this constitutes the main difficulty for solving direct scattering problems. The classical analytical approaches to the problem are based on approximate expressions for this unknown boundary condition. Rigorous approaches, on the other hand, involve the solution of an integral equation for the determination of $F(x_1|\omega)$, and this has to be done numerically. So, the relation between the surface profile function, the conditions of illumination, and the source function is not straightforward.

Consider for a moment a special situation for which the relation between the surface profile function $\zeta(x_1)$ and $F(x_1|\omega)$ is known. Let us further assume that the variation of $\alpha_0(q)$ in Eq. (1) can be neglected. Then, the scattered intensity would be given by the squared modulus of the Fourier transform of the quantity within square brackets. Thus, the phase information of the scattering amplitude has been lost, complicating the inversion of the data. For one-dimensional objects, such as the ones we are considering, it has been demonstrated [18,19] that the reconstruction of a function from the modulus of its Fourier transform does

not yield a unique answer. For our problem, this means that it might be possible to find two or more surfaces that produce the same far-field intensity pattern. Some of these solutions may be trivially related, like an overall vertical shift of the profile, but others may have little correlation with the profile that generated the data.

3 Inverse Scattering as an Optimization Problem

In this section, we formulate the problem of inverse scattering as an optimization problem. It is assumed that we have access to far-field angle-resolved scattered intensity data corresponding to several angles of incidence. The goal is to retrieve the unknown surface profile function from these data. Some constraints on the kind of surface that we seek are introduced in order to reduce the search space.

3.1 The Fitness Function

As we have discussed, although the far-field scattered intensity depends on the surface profile function in a complicated way, the direct problem can be solved fairly rigorously by numerical methods [5]. The closeness of a proposed profile, $z_c(x_1)$, to the original one can be estimated through the difference between the measured angular distribution of intensity, $I^{(m)}(q|k)$, and the angular distribution of intensity, $I^{(c)}(q|k)$, obtained by solving the direct scattering problem with the trial profile $z_c(x_1)$. The goal then would be to find a surface for which the condition $I^{(c)}(q|k) = I^{(m)}(q|k)$ is satisfied. When this happens, and if the solution to the problem is unique, the original profile has been retrieved.

We, thus, define our fitness (objective) function as:

$$f(\zeta(x_1)) = \sum_{i=1}^{N_{\text{ang}}} \int \left| I_s^{(m)}(q|k_i) - I_s^{(c)}(q|k_i) \right| dq, \tag{4}$$

where N_{ang} represents the number of angles of incidence considered, and the $k_i's$ are related to those angles through Eq. (3). Note that in our definition of the fitness function we require that the proposed surface reproduces the "measured" scattering data for several angles of incidence. The satisfaction of this requirement should reduce the number of possible solutions and, hopefully, produce a unique one. The inverse scattering problem can be viewed, now, as the problem of minimizing $f(\zeta(x_1))$.

3.2 Representation and Constraints

To deal with the scattering problem numerically, the surface must be sampled. From the preceding discussion it seems natural to choose the surface heights, evaluated at the sampling points, as the object variables that will change in each iteration of the algorithm. However, changing these numbers independently of each other would lead to surfaces with abrupt height changes, which does not

correspond to the physical situation of interest. One way to avoid this problem is to restrict the search space to randomly rough surfaces that belong to a certain class. We are, thus, faced with a problem of constrained optimization. In our case, we have chosen the target surface as a realization of a stationary, zero-mean Gaussian random process with a Gaussian correlation function.

Surfaces belonging to this class can be generated numerically with the spectral method described in Refs. [4] and [5]. Correlated random numbers that represent the surface heights at the sampling points can be obtained through the expression [5]

$$\zeta_n = \frac{\delta}{\sqrt{L}} \sum_{j=-N/2}^{N/2-1} \frac{[M_j + iN_j]}{\sqrt{2}} \sqrt{g(|q_j|)} \exp\{iq_j\chi_n\}. \tag{5}$$

Here, N represents the total number of points on the surface, L represents its length, $\chi_n = -L/2 + (n - 0.5)\Delta x$ are the sampling points spaced by Δx along x_1, $q_j = -\pi/\Delta x + 2\pi(j - 0.5)/L$ are the sampling points in Fourier space, and $\zeta_n = \zeta(\chi_n)$. The random sets $\{M_j\}$ and $\{N_j\}$ contain statistically independent random Gaussian variables with zero mean and unit standard deviation, and $g(|q_j|)$ represents the power spectral density of surface heights. In order to produce a set of real random numbers $\{\zeta_n\}$, it is required that the complex array $\{M_j + iN_j\}$ be Hermitian. The first and second derivatives of the profile function, which are required for the direct scattering calculations, can be obtained by differentiation of the Eq. (5). The numerical generation of the surface through Eq. (5) is shown, schematically, in Fig. 2. The Fourier transform of the product between the complex array $\{M_j + iN_j\}/\sqrt{2}$ and the square root of the power spectrum of the surface $g(|q_j|)$, produces the real array $\{\zeta_n\}$ that represents the surface heights.

With this notation the fitness function takes the form

$$f(\zeta_n) = \Delta q \sum_{i=1}^{N_{\text{ang}}} \sum_{j=1}^{N_{\text{ff}}} \left| I_s^{(m)}(q_j|k_i) - I_s^{(c)}(q_j|k_i) \right|, \tag{6}$$

where $\Delta q = 2\pi/L$, N_{ff} is the number of far-field angles for which one has data, and the calculated intensity is determined through the expression

$$I_s^{(c)}(q_j|k_i) = \frac{1}{4\alpha_0^2(k_i)} \left| \Delta x \sum_{i=1}^{N} [F_n \exp\{-i\alpha_0(q_j)\zeta_n - iq_j\chi_n\}] \right|^2, \tag{7}$$

where $F_n = F(\chi_n|\omega)$.

The fitness function determines some general properties of the problem that may be useful in the selection of the optimization algorithm. The search space of the function $f(\zeta_n)$ consists of all the random rough surfaces that belong to the specified statistical class. We first note that $f(\zeta_n)$ is N-dimensional with continuous parameters ζ_n. Also, from the form of Eqs. (6) and (7), and the fact that the determination of F_n involves the solution of an integral equation, it is

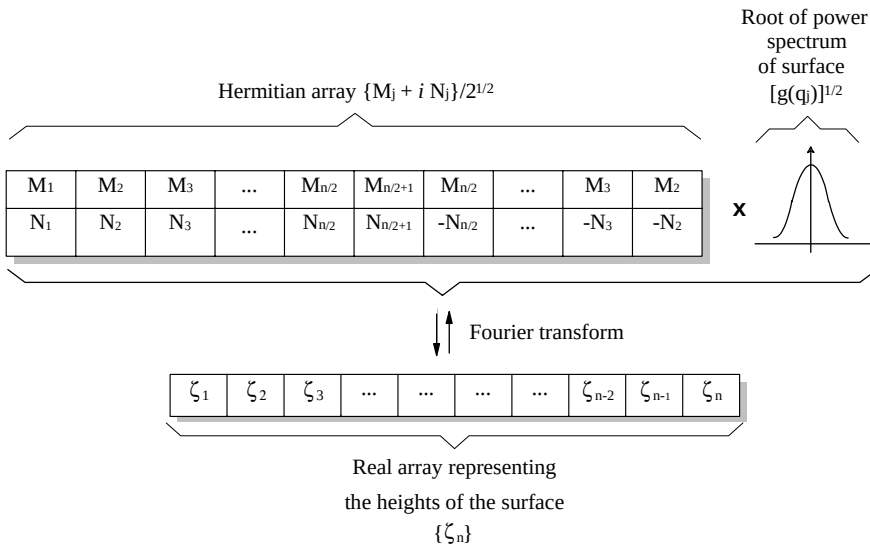

Fig. 2. Illustration of the numerical generation of the random surface.

clear that the derivatives of the fitness function cannot be determined analytically. Furthermore, the numerical evaluation of the derivatives of $f(\zeta_n)$ is not a practical proposition.

3.3 Recombination and Mutation

In the search of the optimum, new trial surfaces related to a previous set of surfaces (population), must be generated. Changes to the old population can be introduced by selectively combining some of these surfaces (recombination), by introducing random changes on them (mutation), or both.

In an intermediate recombination operation, the new surface is the result of a linear combination of Gaussian processes. The result, therefore, is also a Gaussian random processes. However, after the first iteration the surfaces are partially correlated, and the statistics of the resulting surface differ from those of the parent surfaces. In other words, the new generation of surfaces does not belong the statistical class specified for the search space, even though the surfaces of the initial population belong to this class. Thus, if possible, the use of intermediate recombination operations should be avoided.

Mutations, on the other hand, can be introduced by changing some of the elements of the Hermitian array $\{M_l+iN_l\}$ employed in the generation of a given surface [see Fig. 2 and Eq. (5)]. In this case, provided that the new numbers, M_j and N_j, are zero-mean Gaussian-distributed random numbers with unit standard deviation, and the Hermiticity of the array is conserved, the new surface will belong to the statistical class specified for the search space.

4 Description of the Algorithms

In this section, we describe the two evolutionary strategies employed in the search of the optimum. We also discuss, briefly, our first attempts to solve the problem using the downhill simplex method proposed by Nelder and Mead [20,21].

In the simplex method, the number of vertices of the simplex is equal to the dimensions of $f(\zeta_n)$ plus one. Each vertex has an associated value of the fitness function $f(\zeta_n)$, obtained through the evaluation of the $N+1$ random surfaces $\{\zeta_n\}$. In the simplex implementation we explored, a new surface is generated through a reflection operation [21], and the random surface associated with the worst value of $f(\zeta_n)$ is discarded.

We found that the downhill simplex algorithm did not converge to a solution, even after a large number of iterations. Since the reflection operations involved consist of linear combinations of the surface population, the lack of convergence is possibly due to the problem pointed out Sect. 3.3. For this reason, evolutionary strategies were preferred over the simplex method and genetic algorithms. Also, in our the evolutionary strategies, only mutation was used.

Since the time of computation required to find the optimum increases with the number of sampling points on the surface, in order to keep the problem to a manageable size, we chose a surface with $N = 128$ sampling points. To produce a mutation, we first choose randomly some (typically 20) members of the Hermitian array, and substituted them by newly generated numbers with the same statistics. Carrying out the operations illustrated in Fig. 2 [or Eq. (5)] with the new array, we obtain a mutated function profile $\{\zeta_n^{(2)}\}$ that belongs to the same statistical class as the original one. Other mutation schemes can be implemented, but we decided to use the present one due to its relative simplicity.

Using Schwefel's notation [22], the evolutionary strategies explored in this work are the $(\mu + \lambda)$ and the (μ, λ) strategies. In this notation, μ is the number of surfaces in the initial population and λ is the number of surfaces in the population generated through the mutation process. It is worth mentioning that we have previously used λ to denote the wavelength of the light, which is the usual notation in optical work. It is believed that due to the different context in which the two quantities are employed, use of the same symbol to denote both should not lead to much confusion.

In our implementation of the $(\mu + \lambda)$ strategy, we chose $\mu = \lambda$. The first step is the generation of an initial population consisting of μ random surfaces belonging to the specified statistical class. An intermediate population with λ elements is created through the mutation process. From the union of the initial and the intermediate populations we select a secondary population that consists of the μ surfaces with the lowest associated values of $f(\zeta_n)$. This secondary set of surfaces constitutes the starting point for the next iteration of the algorithm. The process continues until the termination criterion is fulfilled, which in our case was set by the maximum number of iterations g.

In the (μ, λ) strategy, we kept $\lambda = 10\mu$ over the entire process. We start with μ random surfaces, and λ new surfaces are generated through the mutation process. The outcome is a secondary population that is evaluated, and from which we

select the μ best random surfaces for the next iteration of the algorithm. As with the $(\mu + \lambda)$ strategy, the process continues until the termination criterion is fulfilled,

5 Results and Discussion

In principle, the data that serves as input to the algorithm should be obtained experimentally. However, in order to study and optimize the algorithms, in these preliminary studies we use data obtained through a rigorous numerical solution of the direct scattering problem [5].

For the two strategies explored, each element of the initial population consisted of a realization of a zero-mean stationary Gaussian-correlated Gaussian random process with a $1/e$-value of the correlation function $a = 2\lambda$ and standard deviation of heights $\delta = 0.5\lambda$. For the $(\mu + \lambda)$ strategy we chose $\mu = \lambda = 100$, whereas for the (μ, λ) strategy we set $\mu = 10$ and $\lambda = 100$. In both cases, the maximum number of iterations was $g = 300$, which also provided the termination criterion. The time of computation is similar with the two algorithms, but the elitist strategy $(\mu+\lambda)$ uses twice as much memory as the non-elitist strategy (μ, λ).

In the numerical experiments we considered five different random profiles to be retrieved. In each case, we used the described algorithms to search for the solution, starting from 30 different initial states chosen randomly. Not in all of the 30 attempts to recover the profile the algorithms converged to the correct one. However, we found that a low value of $f(\zeta_n)$ corresponded, in most cases, to a profile that was close to the original one. So, the final value of $f(\zeta_n)$ was used as the criterion to decide whether the function profile had been reconstructed or not.

For brevity, we only present representative results corresponding to one of the five surfaces studied. The surface profile used to generate the original scattering data is shown in Fig. 3. The surface was sampled at intervals of $\lambda/10$ and contains $N = 128$ points.

The data from which the profile is to be recovered were obtained by illuminating the surface in Fig. 3 from four different directions, defined by the angles of incidence $\theta_0 = -60°$, $\theta_0 = -30°$, $\theta_0 = 0°$, and $\theta_0 = 40°$. In Fig. 4, we show the scattering pattern produced by the surface shown in Fig. 3 for the case of normal incidence.

In Fig. 5 we present results obtained with the two evolutionary strategies we are studying. To facilitate the visualization of the results the original profile is shown in both graphs with a solid line. The vertical displacement of the profile in Fig. 5(a) is quite understandable, as the far-field intensity is insensitive to such shifts. On the other hand, the displacement is unimportant for practical profilometric applications. In this case the two algorithms retrieve the profile quite well; there are only some subtle differences that are perhaps more noticeable near the ends of the surface.

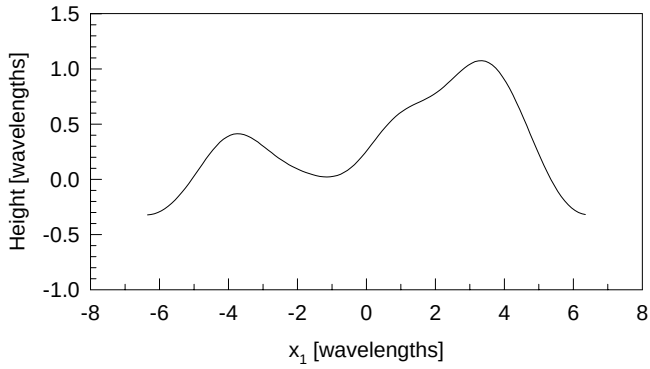

Fig. 3. The profile used in the generation of the scattering data.

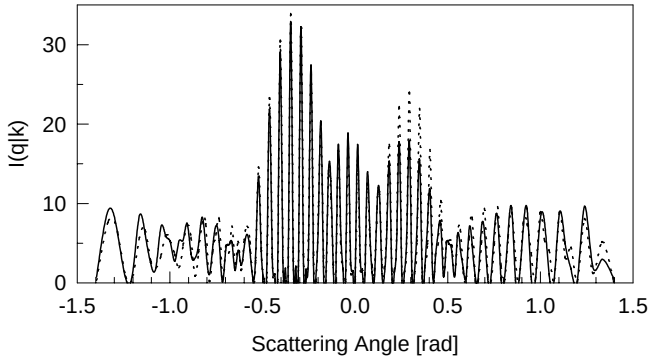

Fig. 4. Scattered intensity produced by the surface depicted in Fig. 3 for the case of normal incidence (solid curve). The dotted curve represents the scattering data produced by the surface shown with the circles in Fig. 6(a) under the same conditions of illumination.

An interesting result that also illustrates the lack of uniqueness of the solution when intensity data are used, is shown in Fig. 6. In Fig. 6(a) we present a curve with the original profile, and a curve with the recovered profile using the (μ, λ) strategy. The initial population differs from the one used in the examples of Fig. 5, with the rest of the parameters being the same. One can see that, in this case, the recovered profile does not resemble the original one.

The scattering patterns, obtained with the two profiles shown in Fig. 6(a) are shown in Fig. 4. The similarity between the two patterns is evident, illustrating the fact that two different profiles can generate scattering data that are practically undistinguishable.

A curious property of the scattering problem is also illustrated in Fig. 6. In Fig. 6(b), we present the profile recovered in Fig. 6(a), reflected with respect of both axis [that is, we replace $z_c(x_1)$ by $-z_c(-x_1)$]. Surprisingly, one observes

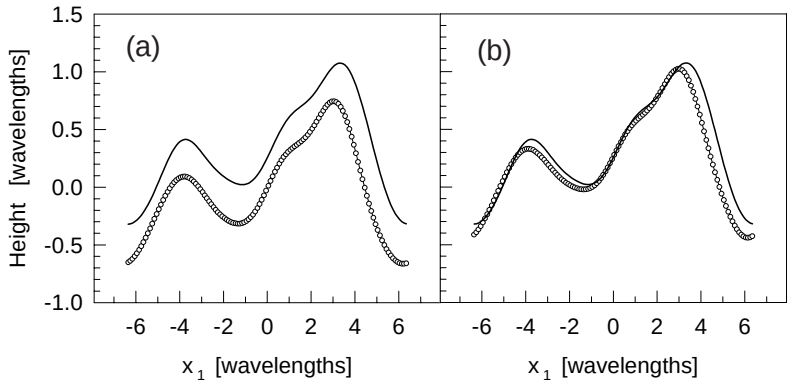

Fig. 5. Reconstruction of the surface profile using (a) the (μ, λ) strategy and, (b) the $(\mu + \lambda)$ strategy. The original profile is plotted with a solid line and the reconstructions are shown by the curves with circles.

that the resulting profile resembles the sought one. It can in fact be shown that in situations in which the polarization effects are not important and the Kirchhoff approximation is valid, the far-field intensity is invariant under this kind of operation [23]. Such situations, which are relatively simple for the direct scattering theories, lead to multiple solutions of the inverse scattering problem. Polarization and multiple scattering effects are then expected to reduce the number of possible solutions to the inverse problem.

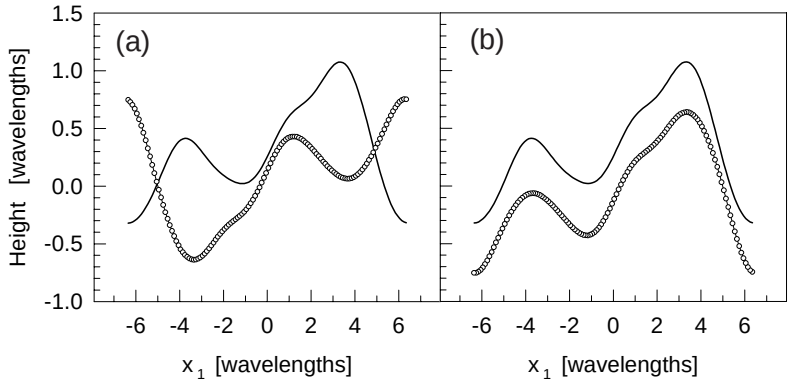

Fig. 6. (a) Reconstruction of the surface profile using the (μ, λ) strategy and a different initial population than in Fig. 5. The original profile is plotted with a solid line and the reconstruction is shown by the curve with circles. (b) Profile representing the profile shown in (a) reflected with respect to both axes (circles). The original profile is shown with a solid line.

6 Summary and Conclusions

We have presented a study of two evolutionary algorithms to solve inverse scattering problems. Starting from far-field intensity data and using both, the $(\mu+\lambda)$ and (μ, λ) strategies, we have successfully retrieved the surface profile that generated the scattering data. The time of computation is similar, but the elitist strategy $(\mu + \lambda)$ uses twice as much memory as the non-elitist strategy (μ, λ).

The solution of the inverse problem is not necessarily unique. We have found that the fitness function has many local minima, and that the initialization of the algorithm plays an important role in the search of the solution. However, in most cases there seems to be a unique global minimum and, in the rare cases in which we have found two solutions, it is possible to perform further tests to decide on the best one. Although the problem has many facets and can be rather complex, the results obtained so far are encouraging.

The success of an inversion scheme based on intensity information opens the possibility of implementing such a procedure experimentally. However, further work is needed, not just regarding the physical aspects of the problem, which have been simplified by our assumptions, but also regarding other aspects related to the performance of the evolutionary algorithms.

Acknowledgments

The authors are grateful to CONACyT (México) for financial support.

References

1. P. Beckmann and A. Spizzichino, *The Scattering of Electromagnetic Waves from Rough Surfaces*, (Pergamon Press, London, 1963), p. 29.
2. J. A. Oglivy, *Theory of wave scattering from random rough surfaces*, (Institute of Physics Publishing, Bristol, 1991), p. 277.
3. Rice, S. O.: Reflection of electromagnetic waves from slightly rough surfaces, Commun. Pure Appl. Math. **4**, 351, 1951.
4. Thorsos, E. I.: The validity of the Kirchhoff approximation for rough surface scattering using a Gaussian roughness spectrum, J. Acoust. Soc. Amer. **83**, 78 (1988).
5. Maradudin, A. A., Michel, T., McGurn, A. R., Méndez, E. R.: Enhanced backscattering of light from a random grating, Ann. Phys. (N. Y.) **203**, 255 (1990).
6. McGurn, A. R., Maradudin, A. A., Celli, V.: Localization effects in the scattering of light from a randomly rough grating, Phys. Rev. B**31**, 4866, 1985.
7. Méndez, E. R., O'Donnell, K. A.: Observation of depolarization and backscattering enhancement in light scattering from Gaussian random surfaces, Opt. Commun. **61**, 91, 1987.
8. Chandley, P. J.: Determination of the autocorrelation function of height on a rough surface from coherent light scattering, Opt. Quant. Electron. **8**, 329, 1976.
9. Welford, W. T.: Optical estimation of statistics of surface roughness from light scattering measurements, Opt. Quant. Electron. **9**, 269, 1977.
10. Chandley, P. J.: Determination of the probability density function of height on a rough surface from far-field coherent light scattering, Opt. Quant. Electron. **11**, 413, 1979.

11. Elson, J. M., Bennett, J. M.: Relation between the angular dependence of scattering and the statistical properties of optical surfaces, J. Opt. Soc. Am. **69**, 31, 1979.
12. Stover, J. C., Serati, S. A.: Calculation of surface statistics from light scatter, Opt. Eng. **23**, 406, 1984.
13. Wombel, R. J., DeSanto, J. A.: Reconstruction of rough-surface profiles with the Kirchhoff approximation, J. Opt. Soc. Am. A **8**, 1892, (1991).
14. Wombel, R. J., DeSanto, J. A.: The reconstruction of shallow rough-surfaces profiles from scattered field data, Inverse Problems **7**, L7, (1991).
15. Quartel, J. C., Sheppard, C. J. R.: Surface reconstruction using an algorithm based on confocal imaging, J. Modern Optics **43**, 496, (1996).
16. Quartel, J. C., Sheppard, C. J. R.: A surface reconstruction algorithm based on confocal interferometric profiling, J. Modern Optics **43**, 591, (1996).
17. Macías, D., Méndez, E. R., Ruiz-Cortés, V.: Numerical study of an inverse scattering algorithm for perfectly conducting one-dimensional surfaces, in *Scattering and Surfaces Roughness*, A. A. Maradudin and Z. H. Gu, eds., Proc. SPIE **4100**, 57-64 (2000).
18. Walther, A.: The question of phase retrieval in optics, Opt. Acta **10**, 41,(1963).
19. O'Neill, E., Walther, A.: The question of phase in image formation, Opt. Acta **10**, 33,(1963).
20. Nelder, J., Mead, R.: A simplex method for function optimization *Computer Journal*, **7**, 308,(1965).
21. Press, W. H. (editor) *Numerical Recipes in Fortran*, (Cambridge University Press, Cambridge, 1992) p. 402.
22. H. P. Schwefel, *Evolution and Optimum Seeking*, (John Wiley & Sons Inc., NY, 1995), p. 444.
23. Macías, D., Méndez, E. R.: Unpublished work (2001).